

PREDICTING THE APPLICATION BEHAVIOR OF  
PRINTING INKS FROM DYNAMIC RHEOLOGICAL  
MEASUREMENTS

Charles L. Rohn

**Abstract:** Realizing that it is not possible to simulate the printing process in the laboratory, it is more logical to decide what rheological measurements and parameters identify the requirements of a good printing ink. The ultimate goal will be to relate the printing quality to the ink formulations.

The steady shear viscosity methods used by the ink technologists to test the flow behavior of printing inks are inadequate. The main reason, as is the case for all dispersions, is that the rheology is strongly dependent on the samples' shear history.

In order to relate the structure of an ink to its composition, it is necessary to make measurements close to a state of rest. This can be accomplished by making low strain dynamic measurements. Furthermore, the response of the ink to controlled shearing over a range of shear rates is needed to relate to its printing quality. Also, the kinetics of structural breakdown and buildup must be measured.

The objective of this paper is to describe a methodology for characterizing printing inks. Four ink samples exhibiting wide ranges in rheological behavior will be discussed in terms of structural differences and applications behavior. In addition to showing strain and frequency dependence of

\*Rheometrics, Inc./Applications

viscoelastic parameters, kinetics of structural breakdown and buildup will also be shown. Furthermore, the relationship of these viscoelastic parameters to tack will be given.

## Introduction

In printing processes, inks must meet a remarkable number of rheological requirements. Coming from the press fountain, the ink must feed properly onto the fountain rollers, distribute, transfer, and suffer structural breakdown, cover the printing form adequately without filling in any of the fine half-tones in pictures. Then it must transfer the image to the paper without serious squash-out. Lastly, it must set on the porous paper sufficiently fast to prevent offset on rollers or paper. All this must be done while the web of paper is moving through the press at speeds up to 25 miles per hour. In a few seconds the ink is compressed, stretched, sheared, fractured, and finally when it meets the paper, it is transferred and set-dried in a fraction of a second.

Furthermore, inks are suspensions that exhibit complex rheological behaviors, such as thixotropy, dilatancy, pseudo-plasticity, and yield stresses. When sheared their structure breaks down, and at rest their structure builds up at varying rates.

Frequently, steady shear viscosity methods are used to characterize the flow behavior of printing inks. This is unsatisfactory because viscosity alone cannot predict the printability of inks. All dispersions, except when very dilute, are viscoelastic. Therefore, it is equally important to measure the inks' elasticity as well as its viscosity.

Dynamic rheological testing provides an excellent means of measuring the viscoelastic parameters of printing inks. These parameters can be related to composition. Once

compositional variable are identified that control viscosity and elasticity independently, it is possible to formulate an ink for optimum printability.

Dynamic rheological data on four printing inks will be discussed and interpreted in terms of their structure. Also, the relationship between complex viscosity and tack will be given.

### Experimental

The Rheometrics Fluids Spectrometer (RFS-8400) was used to measure the dynamic viscoelastic parameters of the inks. These parameters are complex viscosity  $\eta^*$ , storage modulus  $G'$ , and loss modulus  $G''$ . The Appendix defines the physical significance and equations relating to these parameters. Samples were run between 50 millimeter diameter parallel plates. Three different measurements were made: 1) Strain sweep, 2) Frequency sweep, and 3) Step strain. The strain sweep was run from 0.2 percent to 10 percent at a frequency of 40 radians per second. The frequency sweep was run from 0.1 to 100 radians per second and at the following strain. Sample A, 70 percent, sample B, 1.5 percent, sample C, 1.0 percent, and sample D, 0.4 percent. The step strain was performed from 1 percent to 15 percent to 1 percent for samples B, C, D, and 10 percent to 100 percent to 10 percent for sample A. All the step strain measurements were made at 40 radians per second.

Prior to performing the dynamic measurements the samples were subjected to a preshear history. The preshear conditions were one revolution for one minute. By preshearing the reproducibility of repeat measurements were significantly improved. All measurements were made at 25 degrees Celsius.

The tack tests were performed on a

Rheometrics Mechanical Spectrometer (RMS-800) with a 100 gram centimeter normal force transducer. The ink was placed between 50 millimeter diameter parallel plates separated by 1 millimeter. The plates were then pulled apart at a constant speed of 1 centimeter per minute. The force as a function of separation distance was measured, and the maximum value was taken as the tack value.

### Discussion of Results

The first test that is normally run on dispersions is the strain sweep to determine the dependence of the viscoelastic parameters on the degree of strain. Sample A is very strain independent, as shown in Figure 1. Its viscosity is 30 centipoise and it has a very high  $\tan \delta$  of 5.0. This means that this ink has very little structure, which is indicative of a low solids content. Samples B and C show similar  $G'$  and  $G''$  strain dependencies, with sample C having a higher low strain viscosity than sample B, i.e.,  $\eta^*$  (sample C) = 800 centipoise,  $\eta^*$  (sample B) = 500 centipoise. These curves are shown in Figures 2 and 3. Both samples exhibit a linear viscoelastic behavior at low strains. The strain, where  $G'$  becomes strain dependent, is defined as the critical strain  $\gamma_c$ . The apparent yield stress  $\tau_y$  is calculated from the product of the strain independent storage modulus and critical strain. The yield stresses for samples B and C are 2 and 3 dynes per square centimeter, respectively. Also, sample B has a higher  $\tan \delta$  than sample C in the linear viscoelastic region, i.e. 0.64 vs. 0.58. This also means that sample C is more elastic and has a stronger structure.

Sample D, shown in Figure 4, has the most complicated viscoelastic strain dependence. Its viscosity at low strains is about 1800 centipoise. No yield stress is detected and the storage modulus exhibits a minimum and a maximum. This indicates the structure is very

weak, but can build structure at increasing strains. Dispersions that exhibit this type of behavior are composed of weak aggregates that break down into discrete particles. Subsequently, these particles collide and form a quasi-structure, which diminishes with increasing strain.

The frequency dependence of the viscoelastic parameters of structured systems can be separated into three zones: a terminal, plateau, and transition. Figure 5 shows all these zones. The terminal zone is characteristic of the  $\log G'$  and  $\log G''$  vs.  $\log \omega$ , as having slopes of 1 and 2, respectively. Also, the slope dependence of  $\eta^*$  as a function of frequency is zero. Dilute polymeric solutions and dilute, noninteracting dispersions exhibit these characteristics. In these systems the solutes and dispersed phases are moving as discrete domains without interference from their nearest neighbors.

For more concentrated solutions and dispersions, where solute-solute, and particle-particle interactions exist, the slope dependence of  $G'$ , and  $G''$  changes. As the frequency is increased the curves converge and eventually cross. This is where the plateau zone begins. A characteristic feature of the plateau zone is that the magnitude of  $G''$  is smaller than that of  $G'$ . In the plateau region the loss tangent ( $\tan \delta$ ) passes through a minimum. Physically, this zone is the result of topological restraints of the overlapping domains (entanglements) of individual solute molecules or dispersed particles in contact with one another. As the interactions become stronger, the  $\tan \delta$  minimum increases. The width of the plateau zone on the logarithmic frequency scale is related to the distribution of relaxation times associated with the breaking of these topological restraints. This can be viewed from the frequency ranges when  $G'$  and  $G''$  cross each other. The high frequency crossover point is

where the plateau zone ends and the transition zone begins. In the transition zone, the viscoelastic behavior of a concentrated solution or dispersion is dominated by changes on a smaller scale than motions associated with topological restraints. Consequently, these relaxations are independent of the size of the hydrodynamic volume of the solute or particles. They are more directly associated with short range interactions or relaxation within the domains of associated networks.

Sample A, shown in Figure 6, has the lowest viscosity, where  $\eta_0^* = 32$  centipoise. Its viscosity shear rate dependence is negligible. Both terminal slopes of the  $\log G'$ ,  $\log G''$  vs  $\log \omega$ , are close to 2 and 1, respectively. This indicates that the particle interactions are very small and the ink has no structure. The other three ink samples are structured to varying amounts. Figure 7 and 8 shows the plateau moduli. Sample B has the greatest structure as shown by the greatest  $G'$  and lowest  $\tan \delta$  minimum. Also, the breadth of the plateau modulus is the greatest. This indicates that the distribution of relaxation times associated with the topological restraints of the dispersed particles is broader than the other two samples. This could be due to different types of pigments and different distributions of particle sizes. Sample C, shown in Figure 9, exhibits a very similar plateau zone, but has a lower  $G'$  and a higher  $\tan \delta$  minimum. The frequency, where the plateau zone starts, is about 0.1 radian per second for both samples, but the breadth of this zone is greater for sample C. The transition zone for sample B begins at 100 radian per second, and sample C starts well into the next higher decade of frequency. Similarly, sample D exhibits a plateau zone from 0.158 radians per second to 6 radians per second. Also, the transition zone is well defined. This sample has the lowest  $G'$  and highest  $\tan \delta$ . The viscosity-frequency dependence is also different from the other

samples. Not only does it exhibit a strong pseudo-plastic behavior, but it reaches a so called second Newtonian plateau around 50 radians per second.

The next valuable test evaluates time dependence of structural breakdown and structural buildup. This is done by doing the step strain test which is shown in Figures 10-13. For sample A, it is strained for 3 minutes at 10 percent strain, then quickly increased to 100 percent strain, where it was held for 4 minutes, and again returned to 10 percent. All three viscoelastic parameters  $\eta^*$ ,  $G'$ , and  $G''$  are strain independent because the sample exhibited no structural changes. Samples B and C were subjected to about the same step strain conditions of (1 percent to 15 percent to 1 percent). Their rates of breakdown and buildup of structure are identical. When the strain is reduced from 15 percent to 1 percent, the viscoelastic parameters increase slowly over a 5 minute period but do not recover completely. Sample D is very different than all of the other samples. The structure that is broken down at the high strains, recovers so quickly that it overshoots the initial low strain steady state storage modulus  $G'$ . After six minutes this overshoot decays and returns to the low strain modulus.

In view of the predicted printability of these inks, it is obvious that sample A is rheologically the simplest. It is insensitive to variations in strain and strain rates and has no yield stress. As long as the ink does not run excessively at low shear rates, it should perform satisfactorily. The complicated rheology associated with the other three samples could cause printing problems. Sample B and C are very suspect because of their slow rates of structural buildup. This is a major advantage for sample D, whose structural recovery is so fast that it will not run after the stress is removed.

Tack, which is the ability of the ink to resist splitting, was also evaluated. Figure 14 shows force-separation distance for inks sandwiched between two parallel plates. As the plates are spread apart at a constant rate the tack force increases to a maximum. The maximum load is taken as the tack index for the samples. This force ranges between 400 and 600 grams. A correlation between these tack values and low frequency viscosity,  $\eta^*$  (0.1 radians per second) has been found. This is shown in Figure 15. Tack increases exponentially with increasing viscosity. This is expected, providing the tack is measured at low enough frequencies or shear rates.

### Summary

Dynamic rheological measurement provides a valuable means of characterizing the viscoelastic behavior of printing inks. The viscoelastic parameters,  $\eta^*$ ,  $G'$ , and  $G''$  can be used to predict the printability of inks. Furthermore, these parameters relate directly to the structure of dispersed systems and can serve to relate the inks' formulations to their application behavior. Once the components of the formulations are identified that relate to elasticity and viscosity independently, it is possible to optimize the printability of inks. This report also showed that tack is related to the low frequency viscosity of inks. This eliminates the need for doing additional testing to determine this property of inks.

### Appendix

#### Dynamic Rheological Parameters

Dynamic rheological measurements subject a sample to a uniform sinusoidal shear deformation. The instrument strains the sample at a desired frequency (or frequencies) and measures the resulting torque or stress.



The phase angle between the sinusoidal stress and strain waves is also measured and converted into the elastic and viscous moduli of the sample.

The elastic modulus, also called the storage modulus,  $G'$  is obtained from

$$G' = \left( \frac{\sigma^{\circ}}{\gamma^{\circ}} \right) \cos \delta \quad (1)$$

where  $\sigma^{\circ}$  and  $\gamma^{\circ}$  are the maximum stress and strain amplitudes, respectively. The phase angle is  $\delta$ .

The viscous modulus, also called the loss modulus,  $G''$  is obtained from

$$G'' = \left( \frac{\sigma^{\circ}}{\gamma^{\circ}} \right) \sin \delta \quad (2)$$

The complex viscosity is obtained from

$$\eta^* = \frac{\sqrt{(G'(\omega))^2 + (G''(\omega))^2}}{\omega} \quad (3)$$

where  $\omega$  is the frequency in radians/sec.  $\tan \delta$  is obtained from the ratio of  $G''/G'$ .

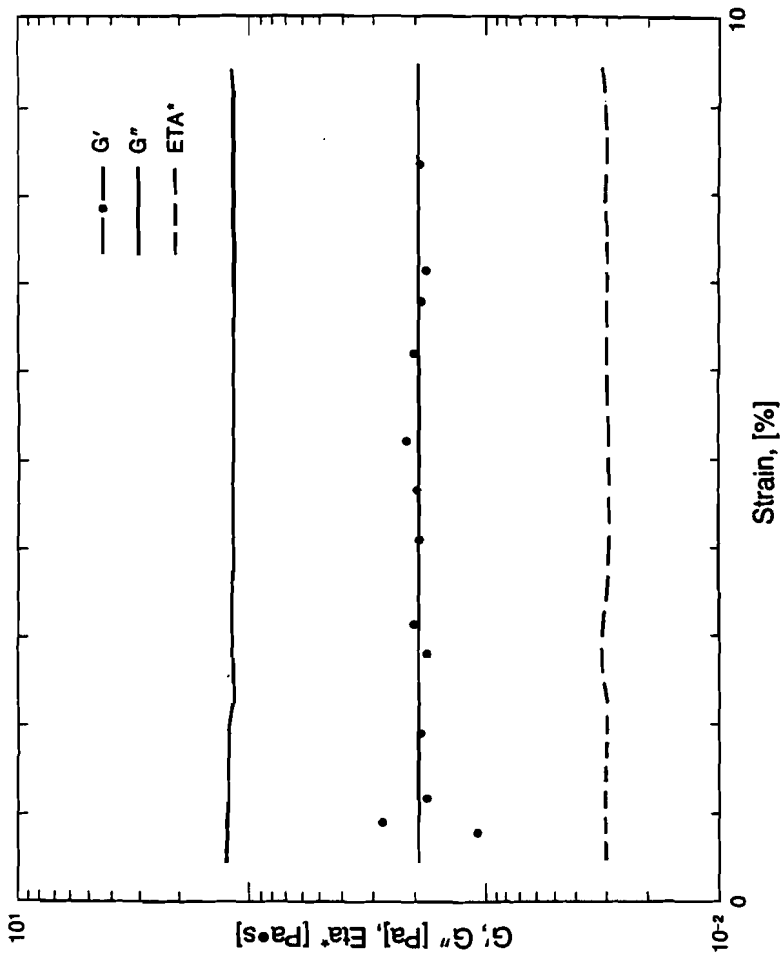


Figure 1

Sample A Strain Sweep

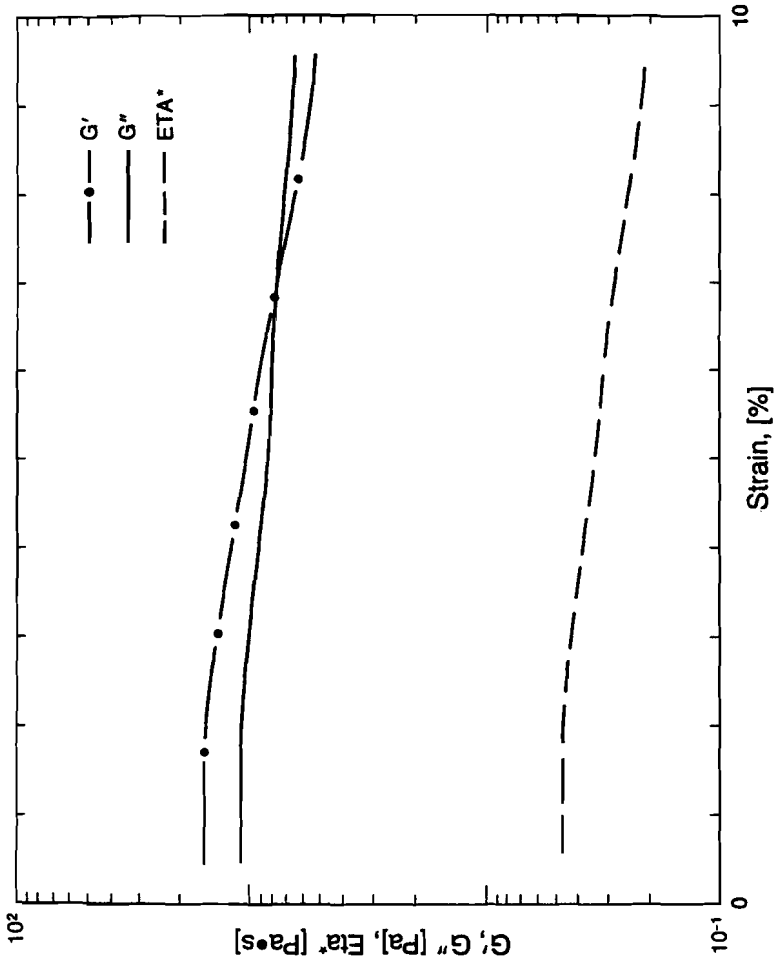


Figure 2

Sample B Strain Sweep

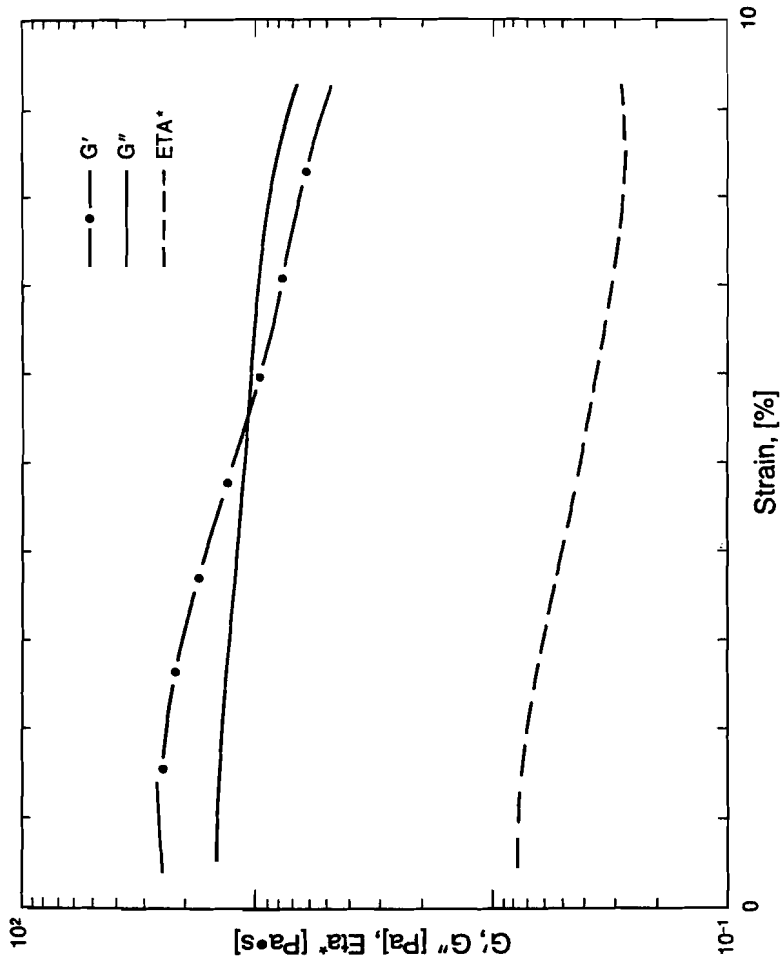


Figure 3  
Sample C Strain Sweep

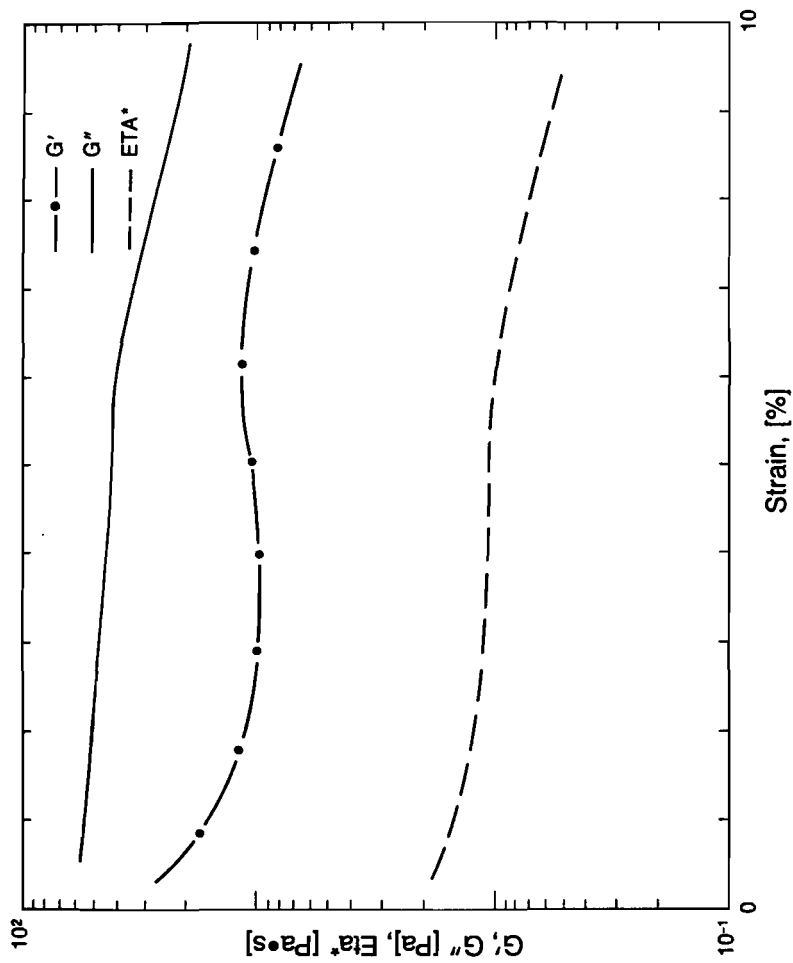


Figure 4

Sample D Strain Sweep

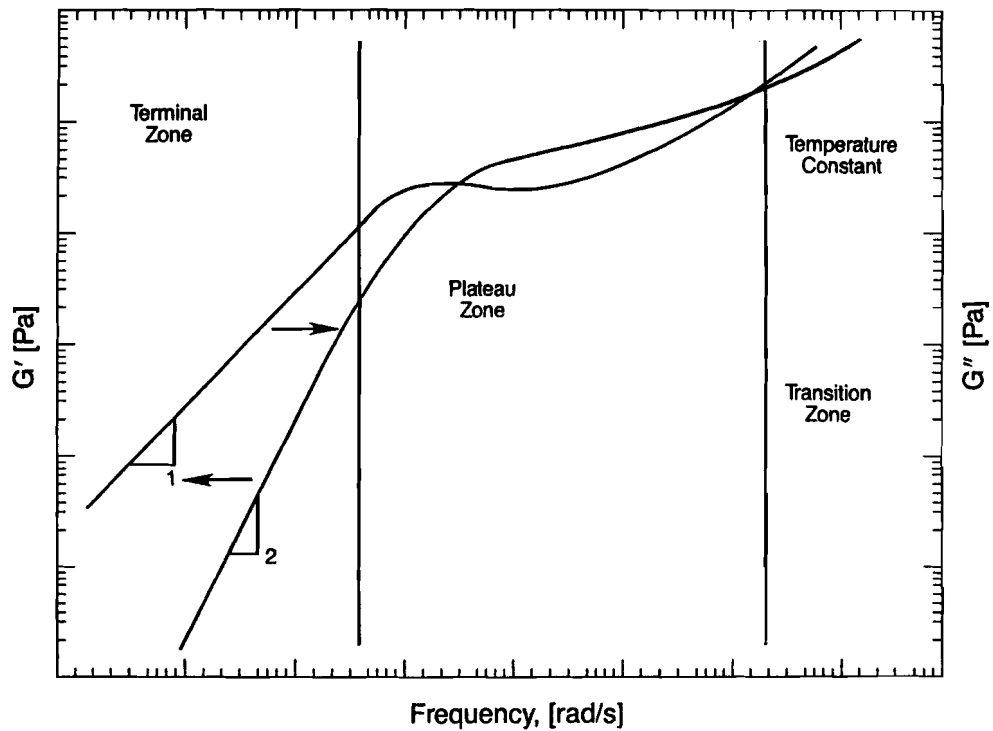


Figure 5

Frequency Dependence of Viscoelastic Parameters

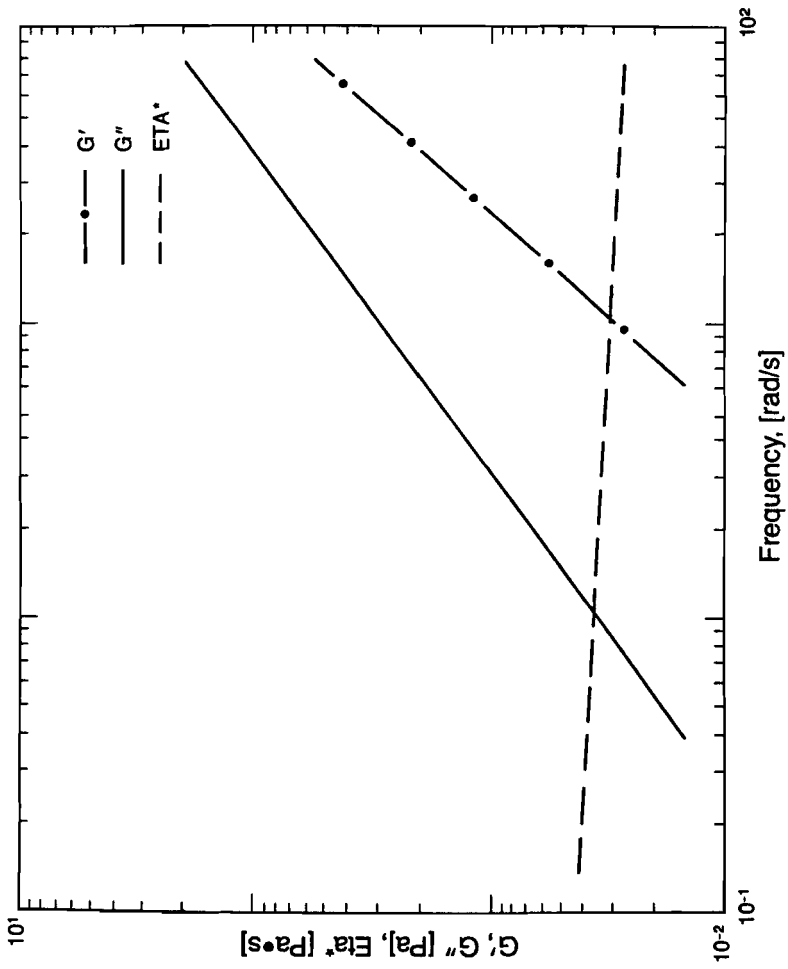


Figure 6

Sample A Frequency Sweep

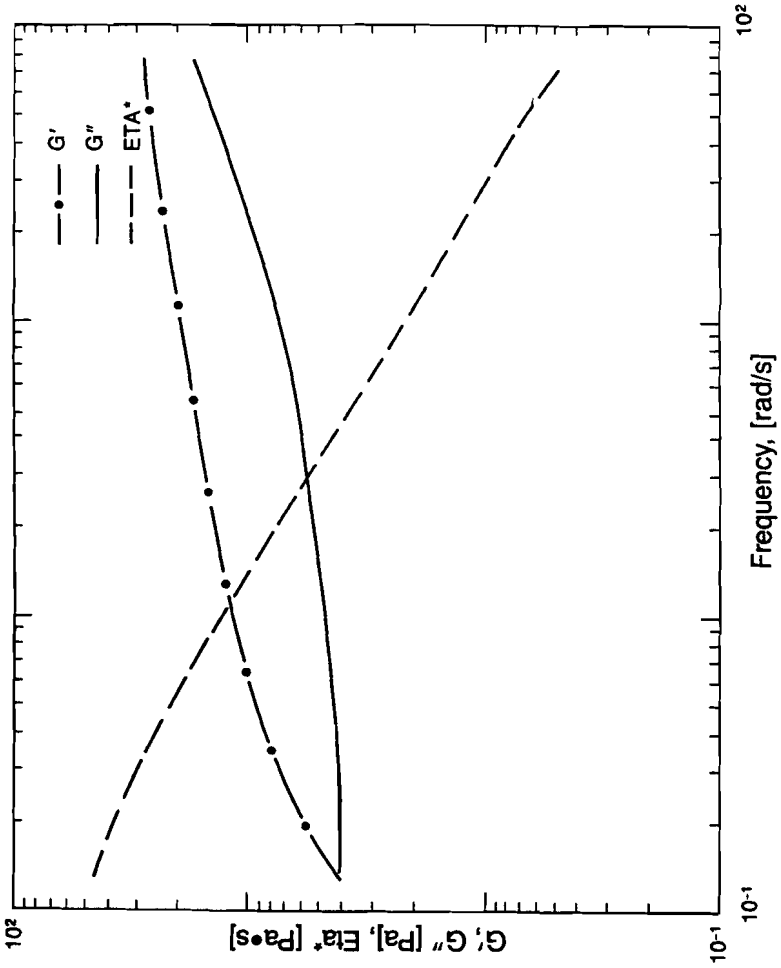


Figure 7

Sample B Frequency Sweep



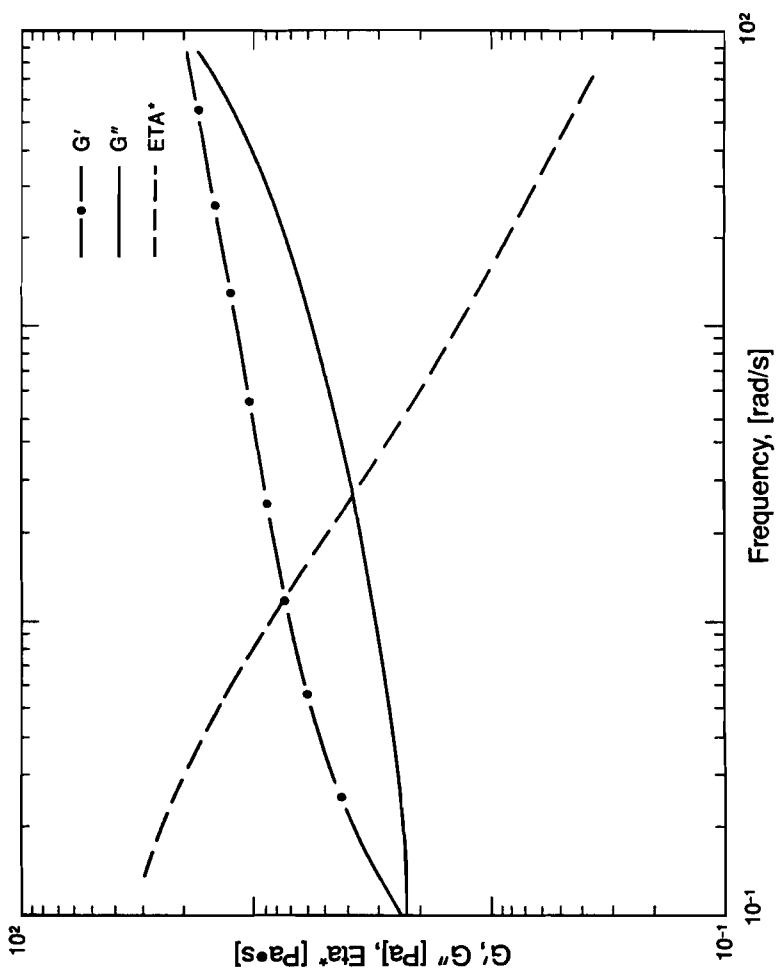


Figure 8  
Sample C Frequency Sweep

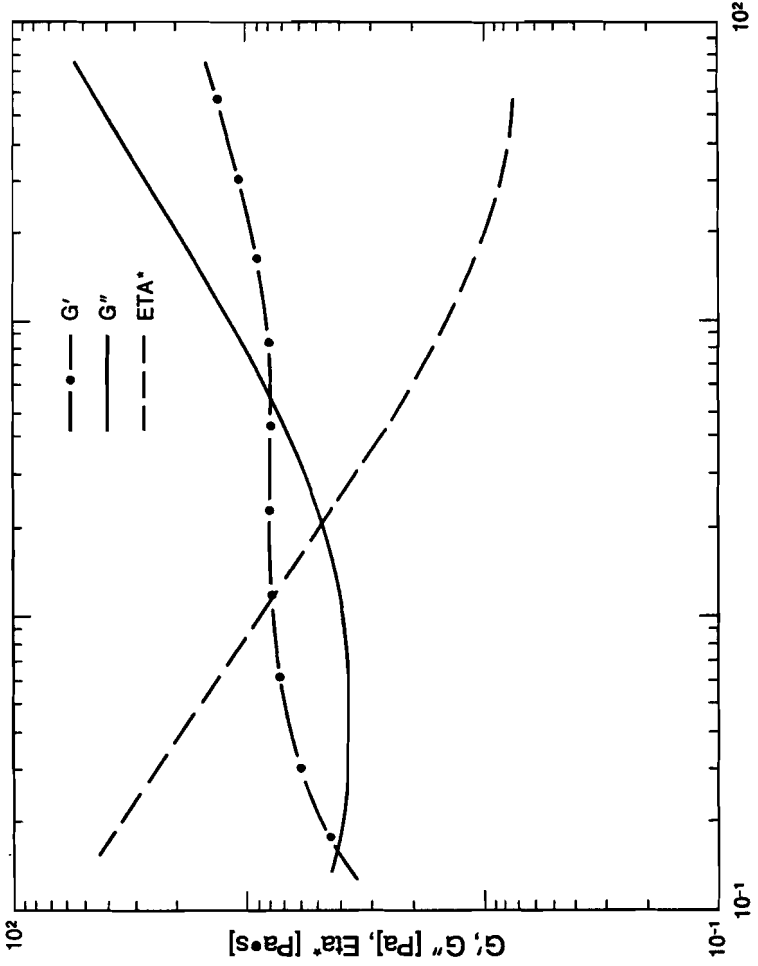


Figure 9  
Sample D Frequency Sweep

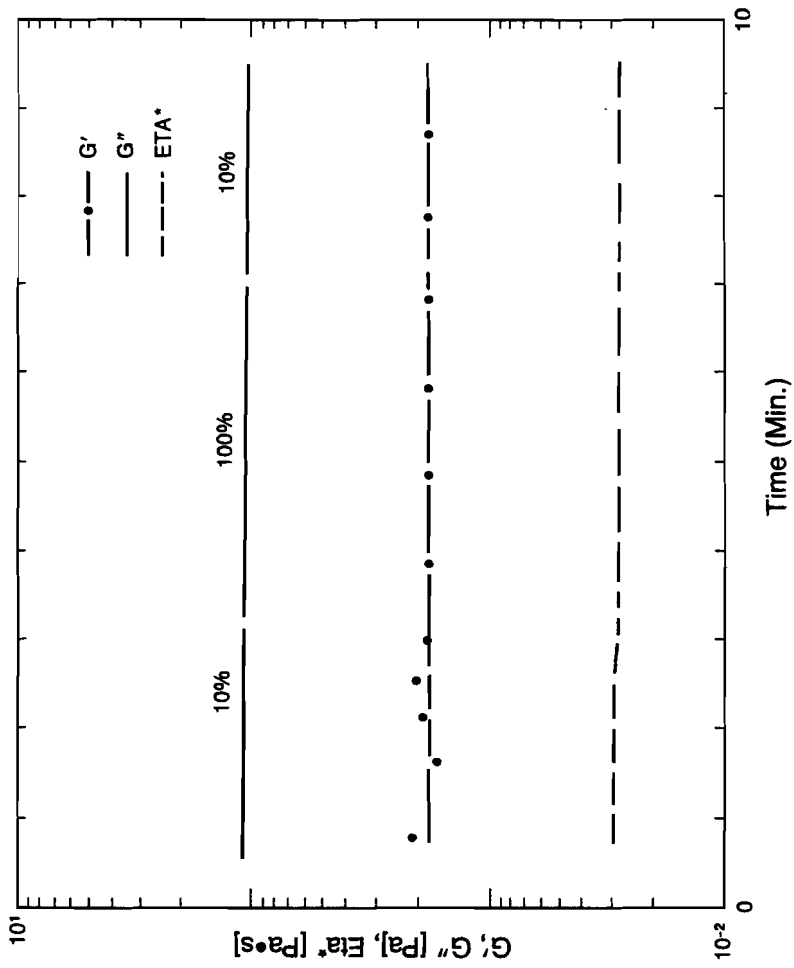


Figure 10  
Sample A Step Strain

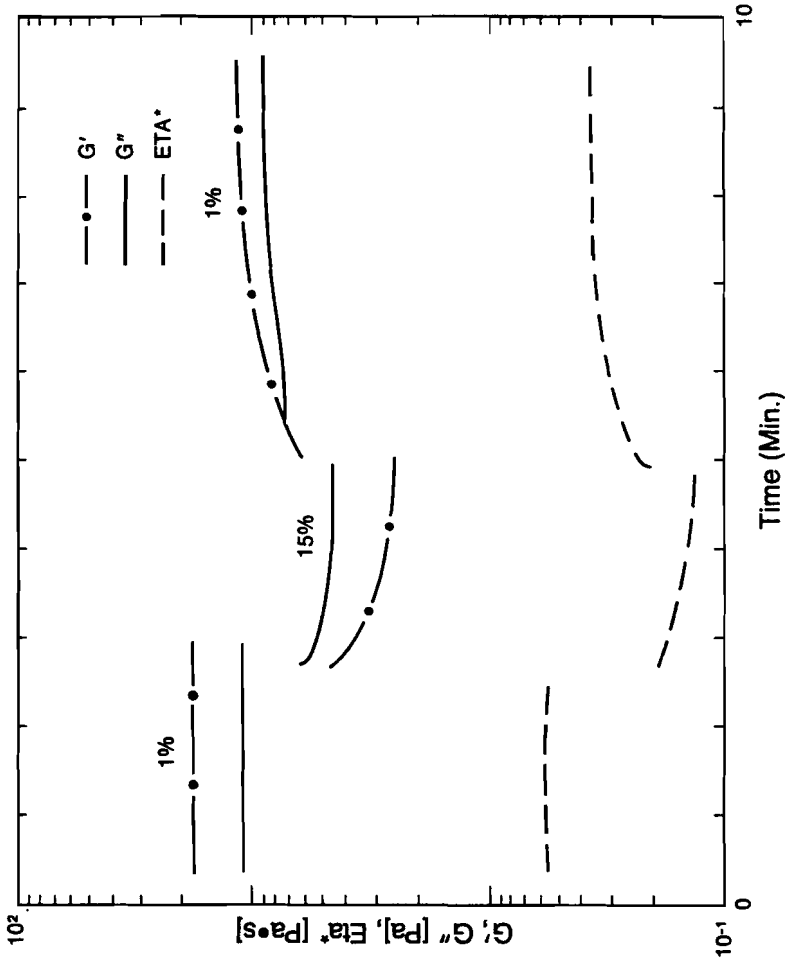


Figure 11

Sample B Step Strain

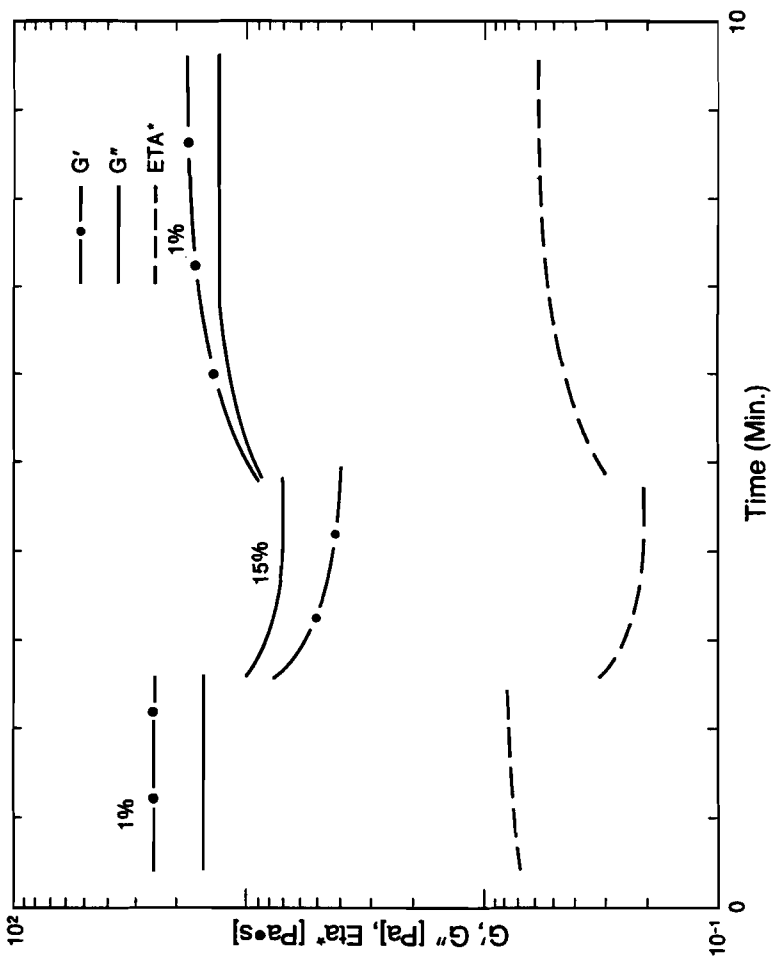


Figure 12

Sample C Step Strain

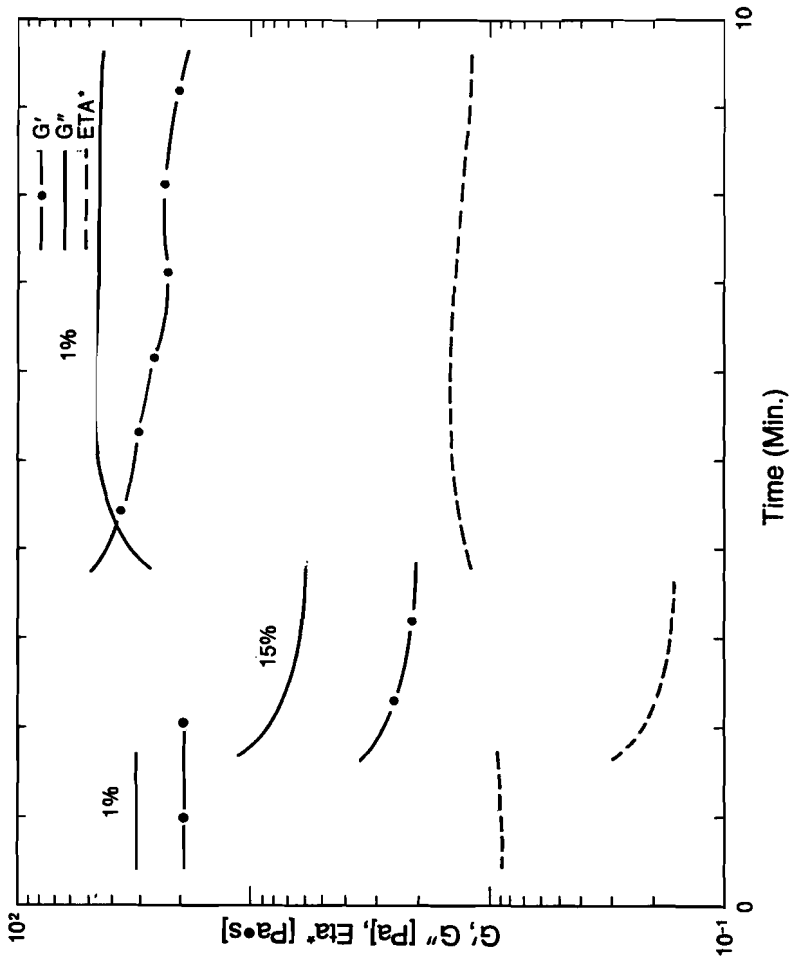


Figure 13  
Sample D Step Strain

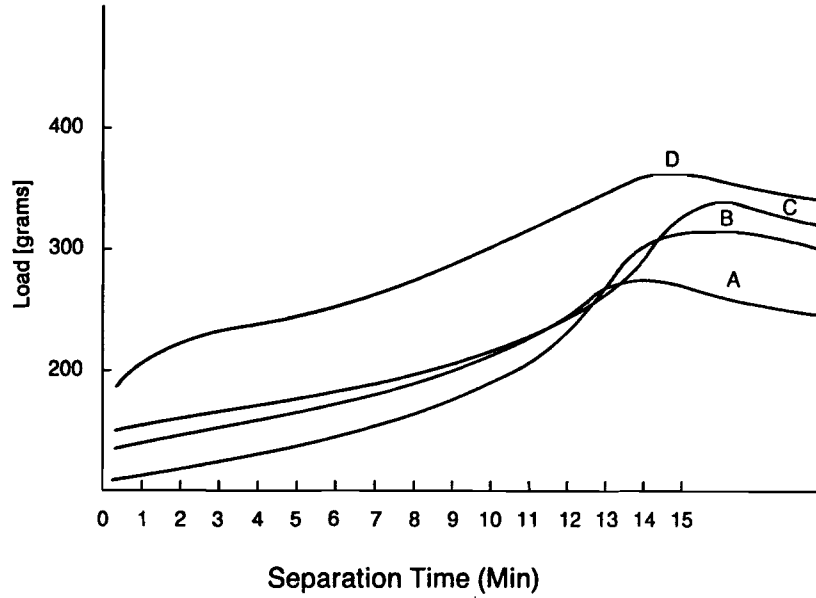


Figure 14

Tack Force vs Separation Time of Plates

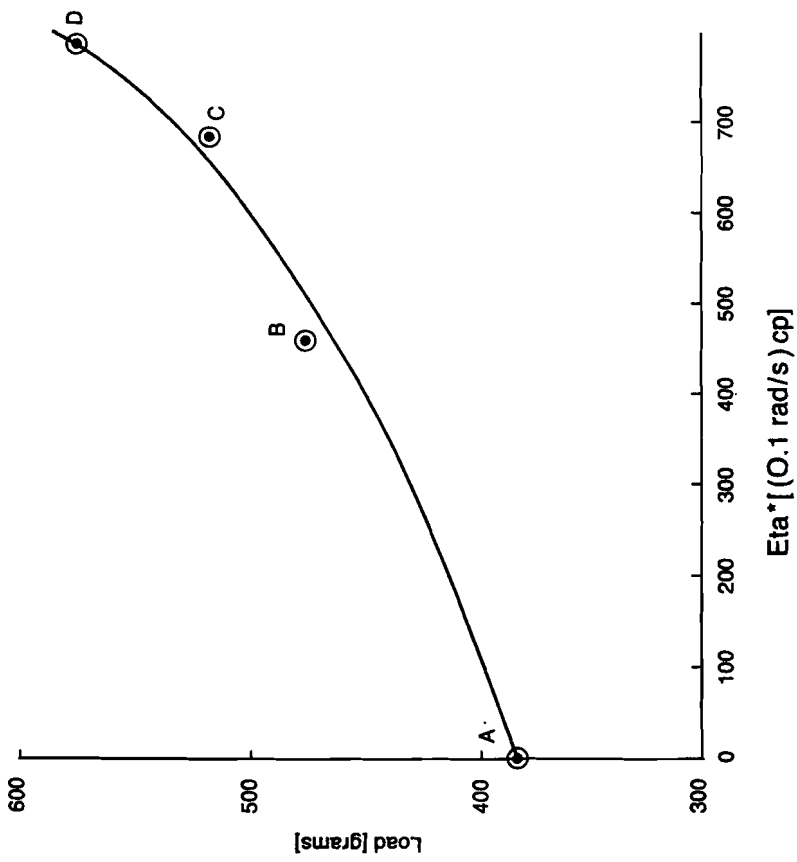


Figure 15  
Tack Force vs Low Frequency Viscosity